Bionatura
Latin American Journal of Biotechnology and Life Sciences

Article

Copper / Chitosan Nanocomposite Prepared by Chemical Method for Active Antimicrobial Activity

Ghufran K. Ibadi [1*], Ali A. Taha[2], and Selma M. H. Al-Jawad[3]

1Biomedical Engineering Department , University of Technology- Iraq. 160006@uotechnology.edu.iq. https://orcid.org/0000-0002-6177-9391
2Biotechnology department, School of Applied Sciences, University of Technology- Iraq. Ali.A.Taha@uotechnology.edu.iq
3Applied physics department, School of Applied Sciences, University of Technology- Iraq. sel-ma.m.aljawad@uotechnology.edu.iq
*Correspondence : 160006@uotechnology.edu.iq

Abstract: Background : Chitosan is a promising polymeric that have received a lot of attention recently. Chitosan nanoparticles have wide applications as a nanocarrier for different organic and inorganic substances. Materials and Methods : In the present study, copper (CuNPs), chitosan nanoparticles (CNPs) and Cu/CS nanocomposite (Cu/CNC) had been prepared and characterized. All prepared nanoparticles were inspected by X-ray diffraction (XRD) , Fourier transform infrared spectroscopy (FTIR), Field emission scanning electron microscope (FE-SEM), Energy Dispersive Spectroscopy (EDS), UV/VIS spectroscopy, and zeta potential. Finally, antimicrobial activity of CuNPs , CNPs and Cu/CNC was tested by disc diffusion assay at different concentrations (0.5-2 mg/ml) against *Candida albicans* , *Klebsiella. pneumoniae* , *Pseudomonas aeruginosa* , *Proteus mirabilis* , *Cryptococcus sp.* , *Staphylococcus aureus*, *Escherichia coli*, and *Acinetobacter sp*. Results :The results showed an absorbance peak at 550 nm due to presence of Cu/CNC. From FTIR spectrum, found peak at 686.66 cm-1 that refers to the copper successfully binding with chitosan. Furthermore, the particle size average of Cu/CNC was 36.34 - 48.27 nm. Cu/CNC have highest growth inhibition zone at concentration 2 mg/ml against *C.albicans*, *P.aeruginosa* and *S.aureus* with the diameters (9.75±0.35, 15±1.41, 15.5±0.70) mm, respectively. Conclution : In this study showed Cu/CNC have high antimicrobial activity than CNPs and CuNPs. It presented high antibacterial activity against gram negative bacteria than gram positive bacteria.

Keywords: Copper nanoparticles, Chitosan nanoparticles, nanocomposite, XRD, FE_SEM Antimicrobial activity.

1. Introduction

Metal nanoparticles (MNPs) are tiny particles made of metal with the size (1-100) nm and it have multiple properties according to the shape, size and composition that determine their catalytic , magnetic and other characteristics such as silver , gold , copper , aluminum , iron ,zinc and other metals [1]. Copper was metal , chemical element, high melting point , high thermal and electrical conductivity , large surface to volume ratio and it converted to copper nanoparticles (CuNPs) by chemical, physical, and biological methods. CuNPs was prepared by chemical method because it is more suitable method, easily reproducible, economical , easily available , require low number of reagents and a reaction temperature close to room temperature should be used [2]. CuNPs were used as antimicrobial, anticancer, agriculture, industrial, medical

and others applications because it have surface Plasmon resonance which appears when it transformed to CuNPs that responsible for inhibiting growth of bacteria and killing of cancer cells [3,4]. CuNPs have antibacterial activity against gram positive and gram negative bacteria by accumulating in the surface of bacterial cell lead to form pores in the membrane then enters the cell. The releases of copper ion in the cell causes damage of DNA and cell death [5,6]. CuNPs are oxidized rapidly and it difficult to synthesis so that used biopolymer as chitosan and others for improving stability of CuNPs [7].

Chitosan is natural polymer obtained from deacetlyation of chitin. It is contain N- acetyl -D-glucosamine and D-glucosamine subunits bounded by β (1,4) glycosidic bonds. It converted to chitosan nanoparticles (CNPs) by Co-precipitation , ionic gelation, micro-emulsion, solvent evaporation and other methods. Due to the low toxicity , biodegradable and biocompatible of CNPs, it can be used in several applications; such as wound healing, photo thermal, antimicrobial, anticancer, and drug delivery [8].

In recent years, many types of literature have reported on the synthesis of CNPs , CuNPs and Cu/CNC. Tyagi *et al.* have studied preparation of chitosan nanoparticles by ionic gelation method then using as antibacterial activity against *E. coli* and *S. aureus* [9]. Resmi *et al*. have studied synthesis of CNPs from extracted shrimp shell waste and used as bactericidal activity against *E.coli* , *Pseudomonas aeruginosa*, *S. aureus* and *S. mutans* [10]. Fatma *et al*. have studied synthesis of copper nanoparticles by green method and it used as antibacterial activity against *E.coli* , *Salmonella typhimurium* and *Acetobacter aceti* [11]. Yaqub *et al*. have studied preparation of CuNPs by chemical method then tested via antimicrobial activity against *E.coli* and *Pseudomonas aeruginosa* [12]. Furthermore, Covarrubias *et al*. have studied synthesis of copper/chitosan nanocomposite for using antibacterial activity against *Streptococcus mutans* [7]. Arjunan *et al*. have studied preparation of Cu/CNC then examined as antimicrobial activity against *Staphylococcus aureus* , *Strepococcus pneumoniae, P.aeruginosa, Proteus vulgaris* and *Candida albicans* [4]. When shown this reports, notices not finding studying about CNPs, CuNPs and Cu/CNC in one report and not studying six strains of bacteria and two strain of fungi. So that, in our research studied synthesis of CNPs, CuNPs and Cu/CNC by chemical method then we identified structural, morphological and optical characterization. Following, CNPs, CuNPs and Cu/CNC was examined as antimicrobial activity against six strains of bacteria (*S. aureus*, *E. coli*, *P. aeruginosa*, *Proteus mirabilis* , *K. pneumonia, and Acinetobacter sp.*) and two strains of fungi (*C. albicans*, *Cryptococcus sp.*) at duplicate with concentrations (0.5, 1, 1.5 and 2) mg/ml by disc diffusion assay.

2. Materials and Methods

2-1 Synthesis of chitosan nanoparticles (CNPs): Chitosan (0.5 g) dissolved in 2% acetic acid under magnetic stirring for 30 min. The gelation solution of dissolved chitosan was sonicated for 10 min at 37 °C. Then 50 ml of methanol was adding by dropper instead of double deionized water and 0.05% of Tween 80 with magnetic stirring at room temperature for 1 hour to form homogenous solution. After obtaining homogenous solution, 0.05% of sodium tripoly phosphate (STTP) was add gradually to chitosan solution under magnetic stirring for 2 hour, and after each 30 min made sonication to disperse nanoparticles. Finally, centrifuged and washed 1-3 until pH reached to (7.0) to obtain pure CNPs.

2-2 Synthesis of copper nanoparticles (CuNPs): CuNPs were synthetized by chemical reduction method. Two grams of starch were dissolved in 100 ml DW under magnetic stirring at 100 °C for 30 min. Then cooled and mixed with mixture of 2 g of copper sulfate, 21g of potassium sodium tartrate and 6 g of NaOH and stirred for 10 min. Thereafter, 10 ml of formaldehyde was added to the mixture with magnetic stirring for 45-60 min until change the color of reaction from blue to brownish red. Then centrifuged, washed 1-3 times until pH reached to 7.0 and dried.

2-3 Synthesis of copper/chitosan nanocomposite (Cu/CNC): Cu/CNC were prepared by dissolving 0.5 g of chitosan in 2% acetic acid and mixed with 0.05 g of CuNPs under magnetic stirring at 80 °C for 1 hour. The solution centrifuged and washed 1-3 times until pH reach 7.0.

2-4Characterization of nanoparticles and nanocomposite: Nanoparticles and nanocomposite were measured by using UV/VIS-specrtophotometry (Schimadzu , Japan) to confirm of nanoparticles formation. FTIR analysis (Schimadzu , Japan) to identify functional groups of NPs in the range 400-4000 cm^{-1}. XRD (Philips , Holanda) to determine structure of particles , zeta potential (Zetasizer Nano , Malvern , UK) to determine stability and surface charge of nanoparticles . FE-SEM (TESCAN, Czech) to identify size and morphology of nanoparticles .EDS analysis to determine chemical elements of nanoparticles.

2-5Antimicrobial activity of nanoparticles and nanocomposite: The antimicrobial activity of nanoparticles and nanocomposite performed by disc diffusion .Antibacterial activity of all nanoforms determined against; *S. aureus , E.coli*, *P. aeruginosa, Proteus mirabilis, K. pneumoniae, Acinetobacter sp.* , on Muller-Hinton agar plates (pH 7), while antifungal activity against *Candida albicans* and *Cryptococcus sp.* were examined on Sabouraud agar (pH 5.6). Moreover, bacterial inoculation size incudes 1.5 $*10^8$ CFU/ml (McFarland standard tube No. 0.5), collected from 24 hours growth cultures , and the optical density at 600 nm (OD_{600}) measured in a spectrophotometer . On the other hand, fungal inoculation size adjusted to $10^6 – 5*10^6$ spores/ ml, obtained from 2-3 days old fungal growth cultures , by microscopic enumeration with cell – counting hematocytometer (Neubauer chamber , Merk , S.A. , Madrid , Spain). The optical density at 530 nm (OD_{530}) of the spores suspension was measured in a spectrophotometer. After media inoculation, a sterilized filter paper disc (6 mm in diameter) was loaded with 20 µl of different NPs or Cu/ CNC in duplicate with concentrations (0.5 , 1 , 1.5 , 2 mg /ml) and placed on the agar surface . The bacterial inoculated plates were incubated at 37 °C for 24 hours, while incubation temperatures of 25 and 30 °C for 24 and 72 hours for both fungal strains, respectively. The diameter of the growth inhibition zone was measured in mm.

3. Results

3.1: Characterization analysis of nanoparticles and nanocomposite

3.1.1: X-Ray diffraction analysis

The crystal structure of nanoparticles and nanocomposite was measured by XRD analysis. In the figure (1) showed XRD of CNPs , CuNPs and Cu/CNC.

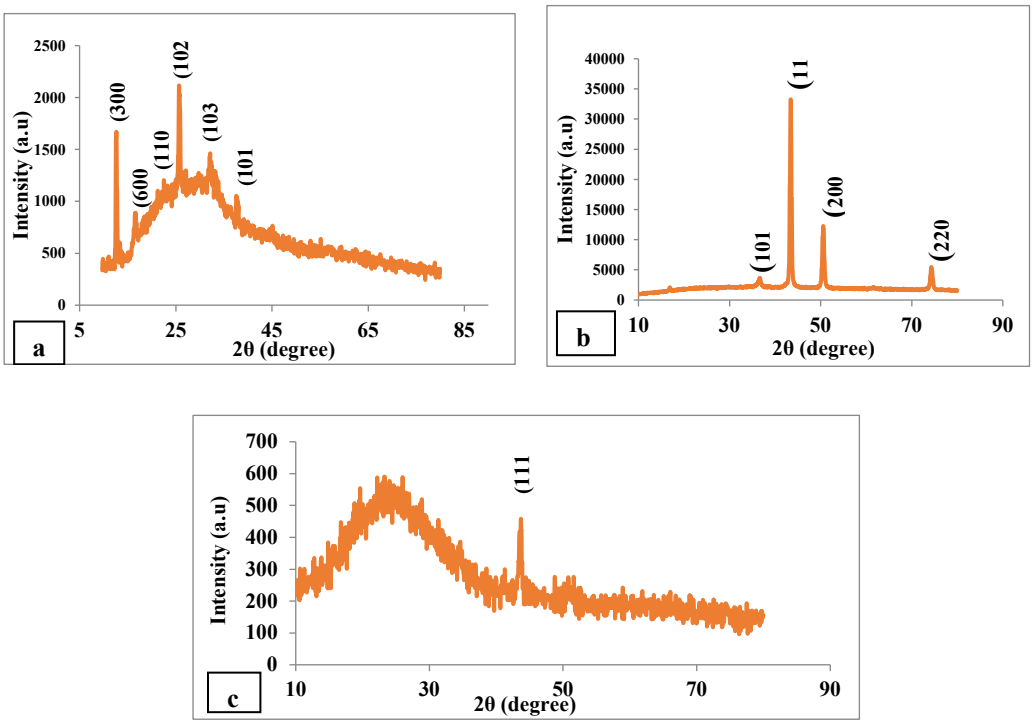

Figure 1 : XRD patterns of (a) CNPs , (b) CuNPs and (c)Cu/CNC.

3.1.2 Fourier Transform Infrared spectroscopy analysis

FTIR spectrum used to determine functional groups of nanoparticles and nanocomposite. The FTIR of CNPs , CuNPs and Cu/CNC as see in the figure (2).

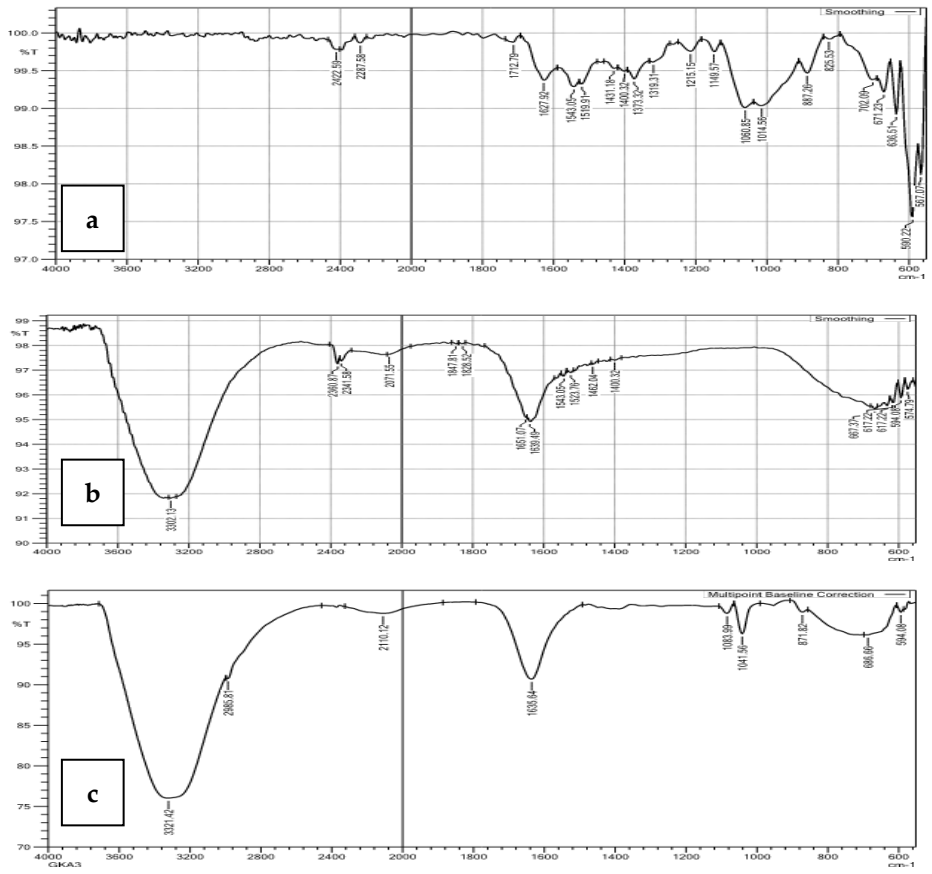

Figure 2 : FTIR spectra of (a) CNPs , (b) CuNPs and (c) Cu/CNC .

3.1.3 : FE-SEM and EDS analysis

FE-SEM used to determine the size and morphology of CNPs , CuNPs and Cu/CNC, as shown in the figure (3). On the other hand, the chemical composition of nanoparticles and nanocomposite were identified by EDS analysis , as shown in the figure (4).

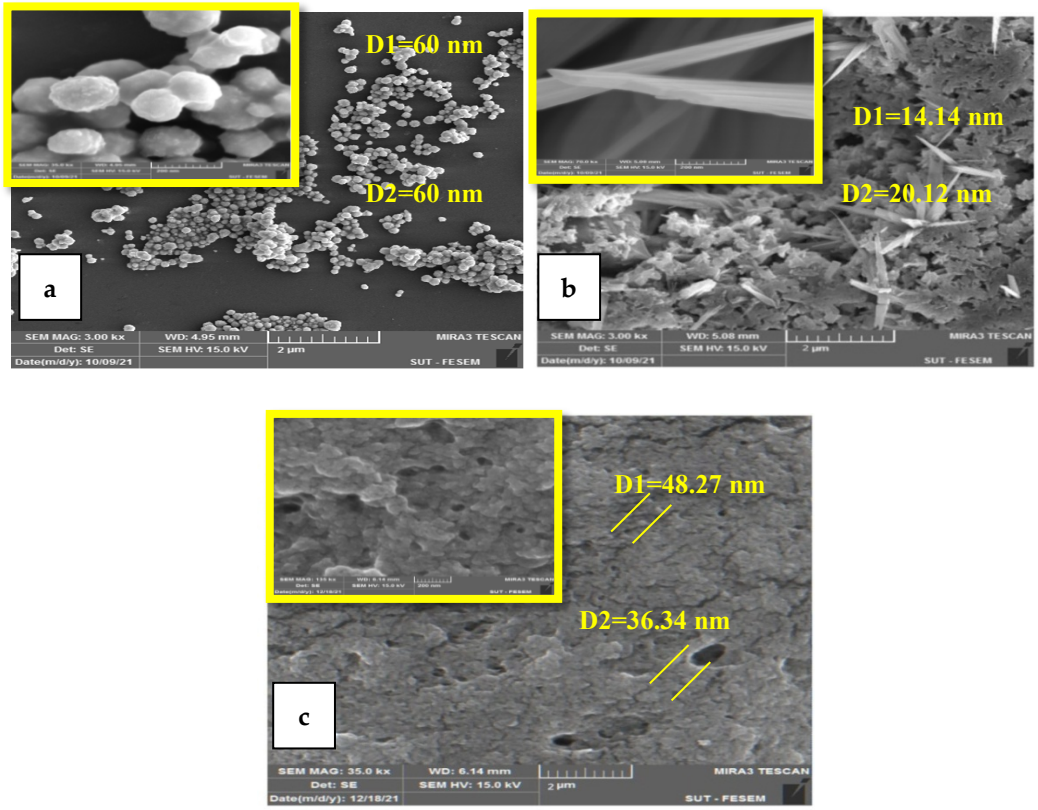

Figure 3 : FE-SEM images of (a) CNPs , (b) CuNPs , (c) Cu/CNC.

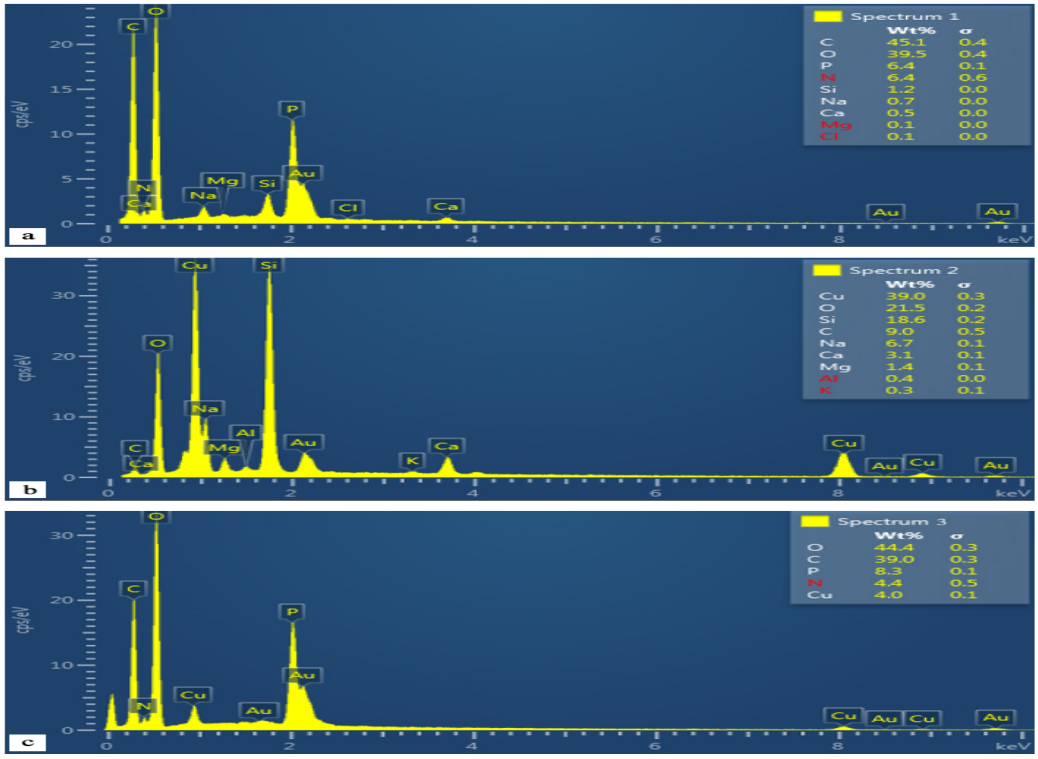

Figure 4 : EDS patterns of (a) CNPs , (b) CuNPs , (c) Cu/CNC.

3.1.5 UV /VIS spectroscopy analysis

The peak absorption of chitosan nanoparticles present at 225 nm and no other optical absorption was appeared. This indicates that the CNPs are pure and these result agreed with those in [13] as shown in the Figure (5a). On the other hand, the absorption peak of CuNPs obtained at 576 nm Figure (5b) that proved the oxidization form and it has strong surface Plasmon resonance (SPR) as determined by[14]. SPR produced from interaction of nanoparticles with the incident light. The free electrons in the copper metal's conduction band oscillate collectively as a result of this interaction. SPR consider spectroscopic property of noble metal nanoparticles that lead to the presence of absorption band in the visible range[15]. Furthermore, absorption peak of Cu/CNC at 540 nm Figure (5c) refers to the chitosan interaction with copper , as mentioned by[4].

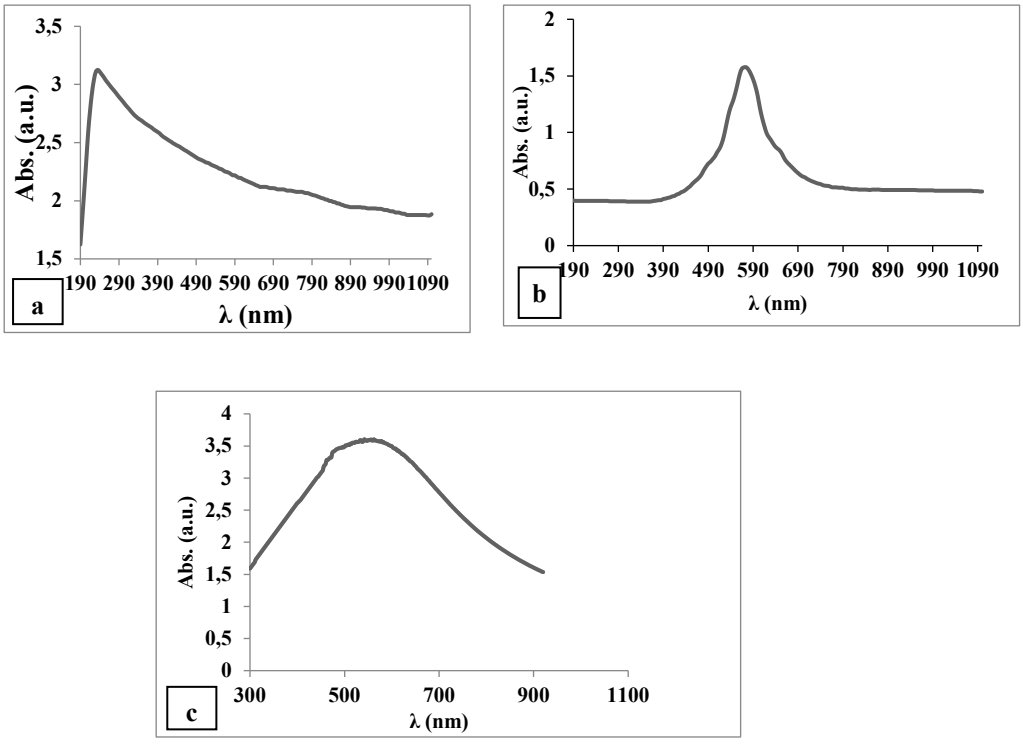

Figure 5 : UV/VIS spectra of (a) CNPs , (b) CuNPs and (c) Cu/CNC.

3.1.6 Zeta potential analyzing

The stability and uniformity of the nano materials were followed up by examining the zeta potential. The zeta potential value of CNPs , CuNPs and Cu/CNC were 10.7 , -44.4 and 15.8 mV respectively, as shown in Figure 6 .

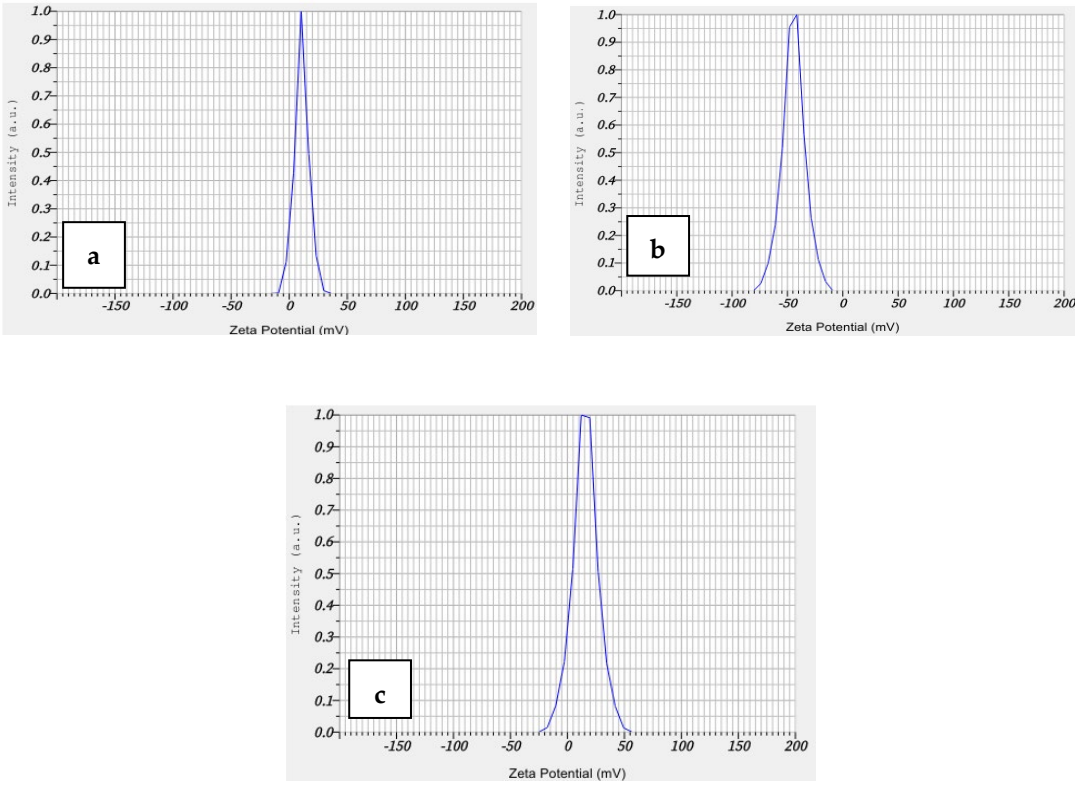

Figure 6 : Zeta potential of (a) CNPs , (b) CuNPs , (c) Cu/CNC.

3.2 Antimicrobial activity of nanoparticles and nanocomposite

CNPs , CuNPs and Cu /CNC were showed inhibitory activity against six bacterial strains (*S. aureus*, *E. coli*, *P. aeruginosa*, *Proteus mirabilis* , *K. pneumoniae* , *Acinetobacter sp.*) and two fungal strains (*C. albicans*, *Cryptococcus sp.*). CNPs and CuNPs were appeared high growth inhibition zone at different concentrations against *C. albicans* followed by *P. aeruginosa* , *K. pneumoniae* , *Proteus mirabilis* , *Cryptococcus sp.* , *S. aureus*, *Acinetobacter sp.* and *E. coli* , as see in the Tables (1,2). The growth inhibition zone caused by Cu/CNC in the presence of bacterial and fungal strains is shown in Tables (1 and 2). The higher growth inhibition zones at concentration 2 mg/ml of 9.75±0.35 , 15±1.41 and 15.5±0.70 mm appeared against *S. aureus, P. aeruginosa* and *C. albicans ,* respectively, but it decreased at concentration 0.5 mg/ml to 7±0 , 7.5±0.70 and 8.25±0.35 mm which refers to when increase concentration of nanoparticles and nanocomposite lead to increase toxicity to bacterial and fungal strains causing growth inhibition and death of cells, as shown in Figures (7-9 C) .

Table (1): The diameters of Gram positive and negative bacteria growth inhibition zone (mm) , mean , standard deviation in the presence of CNPs ,CuNPs and Cu/CNC.

Samples	Con. (mg/ml)	Growth inhibition zone (mm) of											
		S. aureus		*E. coli*		*P.aerogino sa*		*Proteus mirabilis*		*K.pneumo niae*		*Acinetoba cter sp.*	
		Mean	S.D	Mean	S.D	Mean	S.D	Mean	S.D	Mean	S.D	Mean	S.D
CNPs	**0.5**	7	0	6.75	0.35	7.25	0.35	7.5	1.41	7.75	0.35	6.1	0.14
	1	7.5	0	7	0	8.5	2.12	7.1	0.14	8.25	0.35	6.5	0
	1.5	8.1	0.14	7.35	0.07	9	1.41	8.1	0.14	9.25	0.35	7	0
	2	8.5	0.70	7.75	0.07	11	1.41	10.75	0.35	11	1.41	8	0
CuNPs	**0.5**	7.25	0.35	6.5	0	7.5	0.70	6.25	0.35	6.75	0.35	6.1	0.14
	1	7.5	0.70	7	0	9	1.41	6.9	0.56	7.5	0.70	6.3	0.14
	1.5	7.5	0.70	7.75	0.35	10.1	0.14	7.4	0.14	8.8	0.56	6.8	0.28
	2	8.5	0.70	8.25	0.35	12.25	0.35	8.6	0.56	10.6	0.84	7.1	0.14
Cu/CNC	**0.5**	7	0	6.35	0.21	7.5	0.70	7.75	0.35	7.75	0.35	6.15	0.21
	1	7.5	0.70	7.3	0.14	10.5	0.70	8.25	0.35	10.5	0.70	6.4	0.42
	1.5	8	1.41	7.9	0.14	12.5	0.70	8.75	0.35	12	2.82	6.75	0.35
	2	9.75	0.35	8.5	0.14	15	1.41	10.25	1.06	14.5	0.70	7.95	1.20

Table (2): The diameters of fungal strains growth inhibition zone (mm) , mean , standard deviation in the presence of CNPs ,CuNPs and Cu/CNC.

Samples	Concentration (mg/ml)	Growth inhibition zone (mm) of			
		C. albicans		*Cryptococcus sp.*	
		Mean	S.D	Mean	S.D
CNPs	**0.5**	8.75	1.06	6.3	0.42
	1	10.25	0.35	7.45	0.07
	1.5	10.5	0.70	8.3	0.14
	2	12	1.41	9.85	0.91
CuNPs	**0.5**	8	1.41	6.75	0.35
	1	9.5	1.41	7.8	0.28
	1.5	11.5	0.70	8.2	0.28
	2	12.5	0.70	9.15	0.07
Cu/CNC	**0.5**	8.25	0.35	7.15	0.21
	1	10.75	3.18	8.35	0.21
	1.5	12	1.41	9.15	0.21
	2	15.5	0.70	10.5	0.14

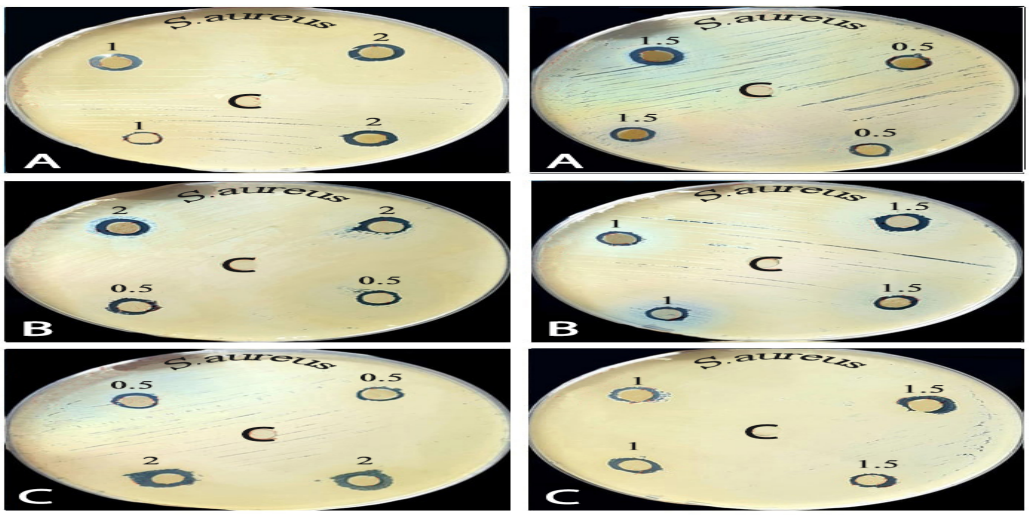

Figure (7): The effect of (A) CNPs, (B) CuNPs and (C) Cu/CNC on *S. aureus*.

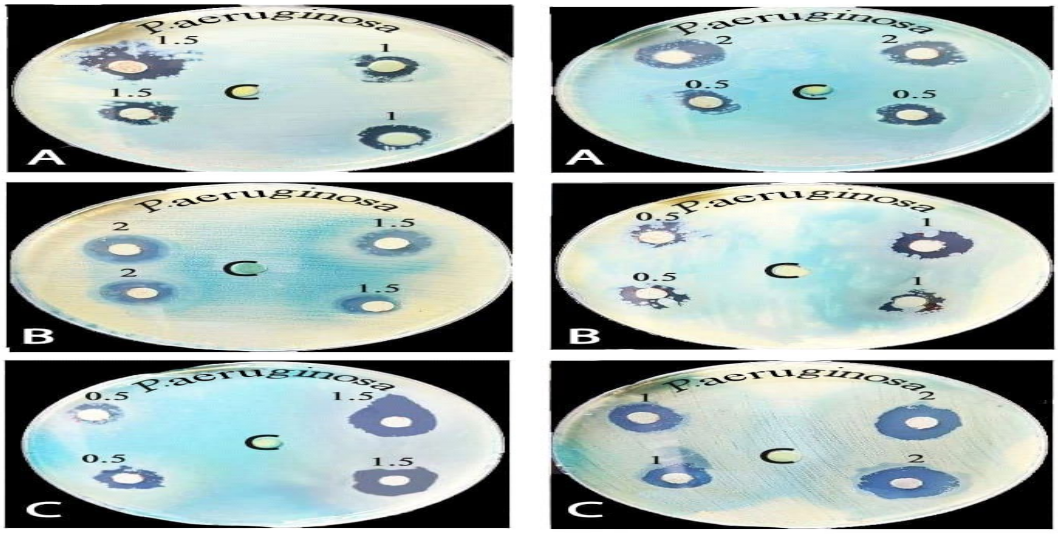

Figure 8: The effect of (A) CNPs, (B) CuNPs and (C) Cu/CNC on *P. aeruginosa*.

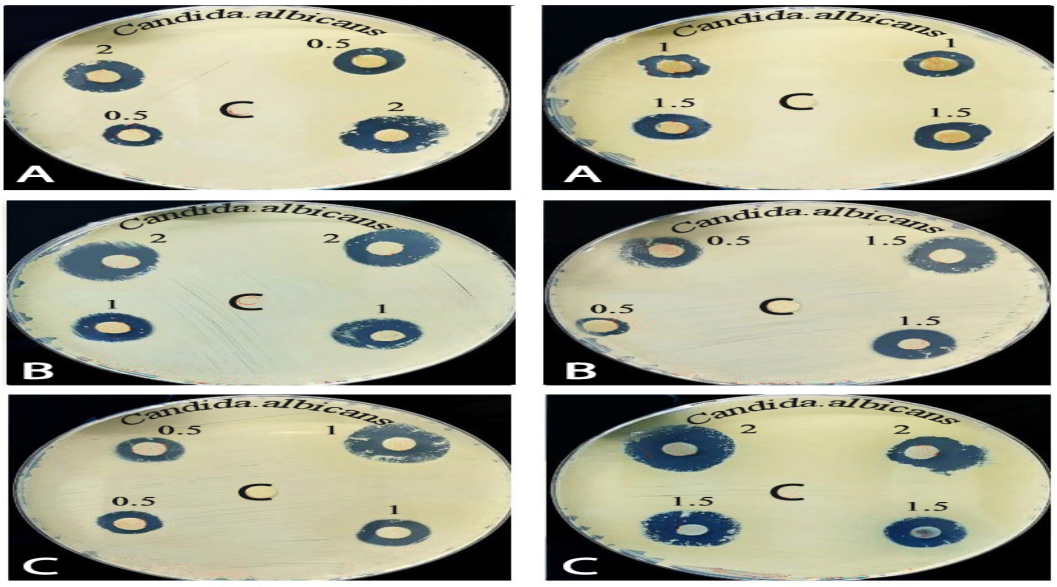

Figure 9: The effect of (A) CNPs, (B) CuNPs and (C) Cu/CNC on *Candida albicans*.

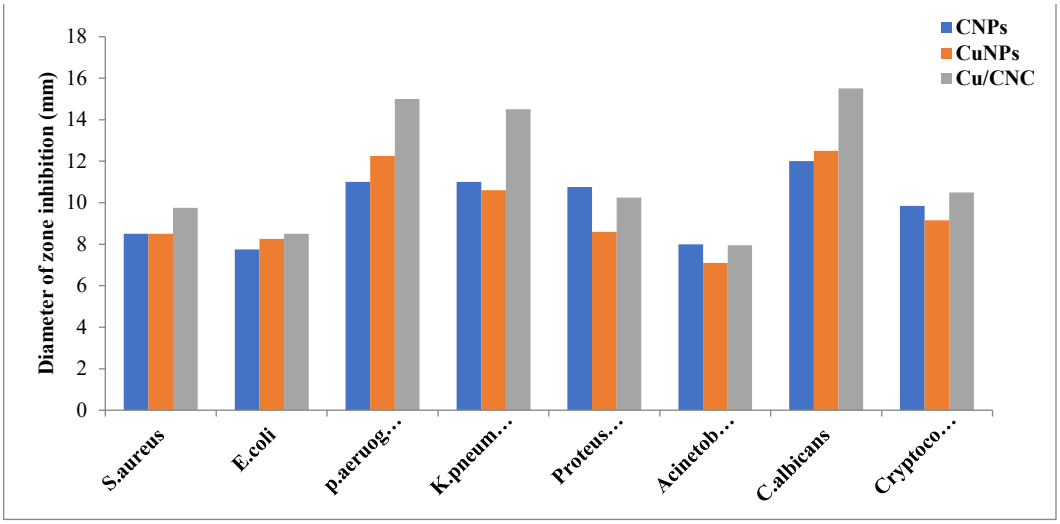

Figure 10 : Antimicrobial activity of CNPs , CuNPs and Cu/CNC at concentrations 2 mg/ml.

4. Discussion

The XRD pattern of chitosan Fig. (1a) was appeared at angles 2θ at 12.5°, 16.5°, 21.5° , 25.9° ,32.5° and 38° corresponding to (300), (600), (110), (210), (103) and (101), this indicate formed crystal of chitosan nanoparticles as matched with [16]. The mean crystallite size of CNPs is 16.65nm that calculated by scheerer's equation (1).

$D = K\lambda / \beta\cos\theta$……(1)

D is crystalline size of nanoparticles, K is 0.154, β is Full Width Half at the Maximum (FWHM) and θ is Bragg angle. On the other hand, XRD pattern of CuNPs Fig.(1b) was observed at angles 2θ = 36.40°, 43.5°, 50.5° and 74.5° corresponding to (101),(111),(200) and(220) that means high nanocrystalline of copper nanoparticles. The average crystallite size of CuNPs is 15.16nm that estimated by scheerer's equation and agreed with[17, 18]. Finally, the XRD pattern of Cu/CNC Fig.(1c) showed a broad peak at 25° which indicated to the chitosan amorphous structure because it interacted with copper nanoparticles. Moreover, peak at 43° in agreement with the plane (111) attributed to crystalline of copper nanoparticles, these result refers to the CuNPs conjugated with CNPs successfully as proved by [19] .

The results of FTIR analysis for chitosan nanoparticles in the Figure (2a) showed that the characteristic peaks of CNPs was at 1543.05 cm-1 and 1627.92 cm-1 refers to amino group and amide I, respectively, while 1519.91 cm-1 indicate the presence of N-H deformation band of chitosan. Moreover, peaks of 1319.31 cm^{-1}, 1215.15 cm^{-1} were due to CH_2 stretching vibration. The bands at 1100-100 cm^{-1} due to the saccharide structure of chitosan , as determined by [17, 20]. On the other hand, FTIR spectra for CuNPs are shown in Figure (2b) , The peak at 3302.13 cm^{-1} indicates stretching vibration of O-H bond , while 1639.49cm^{-1} refers to the stretching vibration of the Cu-O bond of copper oxide nanoparticles. Furthermore, the band at 594.08 cm-1 which attributed to the bending vibration of Cu-O bond and other bands indicate the remains of materials used in the preparation of CuNPs , as obtained by [21]. FTIR analysis of Cu/CNC was shown in the Figure (2c) . The band at 1639.49 cm-1 was decreased to 1635.64 cm-1, while new peak appeared at 2985.81 cm-1 attributed to C-H stretching of chitosan. Moreover, the bands 1651.07 cm-1, 1543.05 cm-1, 1523.76 cm-1, 1462.04 cm-1 and 1400.35 cm1 were deleted from FTIR spectra

of Cu/CNC and finally the peak at 686.66 cm-1 refers to the interaction between copper and chitosan that agreed with results proved by [17, 22].

FE-SEM of CNPs are highly mono dispersed spherical shape nanoparticles with diameter average 60-88 nm, as shown in the Figure (3a). While, the CuNPs image appeared in the form of aggregated crystal cauliflower shape with bundles at the end it, with diameter average 14.14-20.12 nm, this good property for increasing surface to volume ratio of CuNPs for using as antimicrobial that lead to inhibiting growth of bacteria and fungi Figure (3b) [23, 24]. Furthermore, Cu/CNC revealed aggregated, agglomerated and semi-spherical shape with diameter average 36.34-48.27 nm Fig.(3c). The EDS of CNPs show the presence peaks of C, O , P ,N ,Si , Na, Ca and Mg. The presence of nitrogen peak refers to the chitosan formed, as shown in the Figure (4a), that agreed with [25]. Moreover, in the Figure (4b) the EDS of CuNPs exhibit high ratio of Cu and O , that means the copper in oxidized form, as mentioned by [26]. The EDS of Cu/CNC, as shown in Figure (4c), shows peaks of C , O , N , P , and Cu. The presence of nitrogen attributed to the presence of chitosan binding to the CuNPs to form Cu/CNC as proved by [27]. The increase in Zeta potential value refers to the increasing in stability.

In the Fig.6a, the ZP of CNPs was 10.7mV this indicates low stability of chitosan [28], but ZP value of CuNPs was -44.4 mV that means CuNPs had good stability because it oxidized [26], as see in the Fig.6b. Moreover, the ZP of Cu/CNC was 15.8 mV which attributed to increase stability of CNPs when binding with copper [29], as shown in the Fig.6c.

The CNPs showed highest effect of against *S. aureus* and *P. aeruginosa* , as see in the Figures 7 and 8 A. The variance in the results attributed to the difference in the bacterial cell wall , Gram positive have a thick layer of peptidoglycan in their cell wall , which is made of a network having pores that allows foreign particles to enter the cell easily. Whereas, Gram negative have a thin layer of peptidoglycan in their cell wall and an outer membrane made up of lipoprotein, lipopolysaccharide and phospholipid which acts as a strong barrier to foreign particles due to it is bilayer structure [30,31,32]. CuNPs exhibits high antimicrobial activity against *C. albicans, P. aeruginosa and S. aureus*, as see in the Figures (7,8 and 9 B). The diversity of the results refers to various in the bacterial cell wall and CuNPs have high surface to volume ratio so that it precipitated in the cell surface due to form pores in the surface then enters into the cell and release metal ions that causing damage of DNA and death [6,33,34]. Cu/CNC have high antimicrobial activity than CNPs and CuNPs (Fig. 10) which attributed to the positively charged of chitosan interact with the negatively charged of cell surface that enhance the entering of NPs into cell and release metal ions that block intracellular components and caused cell death [35,36,37].

5. Conclusions

Cu/CNC were successfully prepared by simple and low cost method then characterized. Cu/CNC appeared as semi-spherical in shape with low stability. Antimicrobial activity of Cu/CNC was higher than CNPs and CuNPs. Antibacterial activity of Cu/CNC was higher against gram negative than gram positive strains. C. albicans looked more sensitive to the Cu/CNC among all examined fungal and bacterial strains used in the present study.

Ethics approval : None required.

Conflict of interest : None declared.

Funding : No funding.

Acknowledgments : Our appreciation and gratitude to the department of applied sciences at the University of Technology, Iraq.

References

1. Huynh, K. H., Pham, X. H., Kim, J., Lee, S. H., Chang, H., Rho, W. Y., & Jun, B. H. Synthesis, properties, and biological applications of metallic alloy nanoparticles. *International Journal of Molecular Sciences*, **2020**, *21*(14), 5174.
2. Venkatesh, N., Bhowmik, H., & Kuila, A. Metallic nanoparticle: a review. *Biomedical Journal of Scientific & Technical Research*, **2018**, *4*(2), 3765-3775.
3. Khandel, P., & Shahi, S. K. Microbes mediated synthesis of metal nanoparticles: current status and future prospects. *Int J Nanomater Biostruct*, **2016**, *6*(1), 1-24.
4. Arjunan, N., Singaravelu, C. M., Kulanthaivel, J., & Kandasamy, J. A. potential photocatalytic, antimicrobial and anti-cancer activity of chitosan-copper nanocomposite. *International journal of biological macromolecules*, **2017**, *104*, 1774-1782.
5. Tamilvanan, A., Balamurugan, K., Ponappa, K., & Kumar, B. M. Copper nanoparticles: synthetic strategies, properties and multifunctional application. *International Journal of Nanoscience*, **2014**, *13*(02), 1430001.
6. Din, M. I., Arshad, F., Hussain, Z., & Mukhtar, M. Green adeptness in the synthesis and stabilization of copper nanoparticles: catalytic, antibacterial, cytotoxicity, and antioxidant activities. *Nanoscale research letters*, **2017**,*12*(1), 1-15.
7. Covarrubias, C., Trepiana, D., & Corral, C. Synthesis of hybrid copper-chitosan nanoparticles with antibacterial activity against cariogenic Streptococcus mutans. *Dental materials journal*, **2018**,*37*(3), 379-384.
8. AL- Shamary, W. A. .; Alkhateb, B. A. A. H. .; Abdel, E. T. . Role Of Perlite Quantity And Intervals Of Irrigation On Potatoes (Solanum Tuberosum L.) Grown In Gypsiferous Soil. *Journal of Life Science and Applied Research*. **2020**, 1, 31-39.
9. Tyagi, A., Agarwal, S., Leekha, A., & Verma, A. K. Effect of mass and aspect heterogeneity of chitosan nanoparticles on bactericidal activity. *Int. J. Adv. Res*,**2014**, *2*(8), 357-367.
10. Resmi, R., Yoonus, J., & Beena, B. Anticancer and antibacterial activity of chitosan extracted from shrimp shell waste. *Materials Today: Proceedings*,**2021**, *41*, 570-576.
11. Fatma, S., Kalainila, P., Ravindran, E., & Renganathan, S. Green synthesis of copper nanoparticle from Passiflora foetida leaf extract and its antibacterial activity. *Asian Journal of Pharmaceutical and Clinical Research*, **2017**, 79-83.
12. A. Yaqub, N. Malkani, A. Shabbir, S. A. Ditta, F. Tanvir, S. Ali, M. Naz, S. A. R. Kazmi, and R. Ullah, "Novel Biosynthesis of Copper Nanoparticles Using Zingiber and Allium sp. with Synergic Effect of Doxycycline for Anticancer and Bactericidal Activity," Current Microbiology, **2020**, vol. 77, no. 9, pp. 2287–2299, Jun.
13. Agarwal, M., Agarwal, M. K., Shrivastav, N., Pandey, S., Das, R., & Gaur, P. Preparation of chitosan nanoparticles and their in-vitro characterization. *International Journal of Life-Sciences Scientific Research*, **2018**, *4*(2), 1713-1720.
14. Mohamed, E. A. Green synthesis of copper & copper oxide nanoparticles using the extract of seedless dates. *Heliyon*, **2020**, *6*(1), e03123.
15. Ibraheem M W, AL Mjbel A A, Abdulwahid A S, Mohammed Th. T. Characterization of the influence of diet on Japanese quail. *Revis Bionatura*. **2022**;7(4) 21. http://dx.doi.org/10.21931/RB/2022.07.04.21.
16. Thamilarasan, V., Sethuraman, V., Gopinath, K., Balalakshmi, C., Govindarajan, M., Mothana, R. A., ... & Benelli, G. Single step fabrication of chitosan nanocrystals using Penaeus semisulcatus: Potential as new insecticides, antimicrobials and plant growth promoters. *Journal of Cluster Science*, **2018**, *29*(2), 375-384.
17. Usman, M. S., El Zowalaty, M. E., Shameli, K., Zainuddin, N., Salama, M., & Ibrahim, N. A. Synthesis, characterization, and antimicrobial properties of copper nanoparticles. *International journal of nanomedicine*, **2013**, *8*, 4467.
18. AL-Jawad, S. M., Shakir, Z. S., & Ahmed, D. S. Antibacterial activity of Nickel-doped ZnO/MWCNTs hybrid prepared by sol–gel technique. *The European Physical Journal Applied Physics*, **2021**,*96*(2), 21201.

19. Ebrahimiasl, S., & Younesi, S. A. Shelf Life Extension of Package's Using Cupper/(Biopolymer nanocomposite) Produced by One-Step Process. *Journal of Food Biosciences and Technology*, **2018**, *8*(1), 47-58.
20. Huseen, R. H., Taha, A. A., Ali, I. Q., Abdulhusein, O. M., & Al-Jawad, S. M. Biological activity of gum Arabic-coated ferrous oxide nanoparticles. *Modern Physics Letters B*, **2021**, *35*(24), 2150411.
21. Raul, P. K., Senapati, S., Sahoo, A. K., Umlong, I. M., Devi, R. R., Thakur, A. J., & Veer, V. CuO nanorods: a potential and efficient adsorbent in water purification. *Rsc Advances*, **2014**, *4*(76), 40580-40587.
22. Alghamdi, K. S., Ahmed, N., Bakhotmah, D., & Mokhtar, M. Chitosan Decorated Copper Nanoparticles as Efficient Catalyst for One-Pot Multicomponent Synthesis of Novel Quinoline Derivatives: Sustainable Perspectives, **2018**.
23. Barbari, G. R., Dorkoosh, F. A., Amini, M., Sharifzadeh, M., Atyabi, F., Balalaie, S., ... & Tehrani, M. R. A novel nanoemulsion-based method to produce ultrasmall, water-dispersible nanoparticles from chitosan, surface modified with cell-penetrating peptide for oral delivery of proteins and peptides. *International journal of nanomedicine*, **2017**, *12*, 3471.
24. Ruman, U., Buskaran, K., Pastorin, G., Masarudin, M. J., Fakurazi, S., & Hussein, M. Z. Synthesis and characterization of chitosan-based nanodelivery systems to enhance the anticancer effect of sorafenib drug in hepatocellular carcinoma and colorectal adenocarcinoma cells. *Nanomaterials*, **2021**, *11*(2), 497.
25. Rafigh, S. M., & Heydarinasab, A. Mesoporous chitosan–SiO2 nanoparticles: synthesis, characterization, and CO2 adsorption capacity. *ACS Sustainable Chemistry & Engineering*, **2017**, *5*(11), 10379-10386.
26. Al-Zharani, M., Qurtam, A. A., Daoush, W. M., Eisa, M. H., Aljarba, N. H., Alkahtani, S., & Nasr, F. A. Antitumor effect of copper nanoparticles on human breast and colon malignancies. *Environmental Science and Pollution Research*, **2021**, *28*(2), 1587-1595.
27. Hongfeng, Z., El-Kott, A., Ahmed, A. E., & Khames, A. Synthesis of chitosan-stabilized copper nanoparticles (CS-Cu NPs): Its catalytic activity for CN and CO cross-coupling reactions and treatment of bladder cancer. *Arabian Journal of Chemistry*, **2021**, *14*(10), 103259.
28. Gatta, A. K., Chandrashekhar, R., Udupa, N., Reddy, M. S., Mutalik, S., & Josyula, V. R. Strategic Design of Dicer Substrate siRNA to Mitigate the Resistance Mediated by ABCC1 in Doxorubicin-resistant Breast Cancer. *Indian Journal of Pharmaceutical Sciences*, **2020**, *82*(2), 329-340.
29. Bandara, S., Carnegie, C. A., Johnson, C., Akindoju, F., Williams, E., Swaby, J. M., ... & Carson, L. E. Synthesis and characterization of Zinc/Chitosan-Folic acid complex. *Heliyon*, **2018**,*4*(8), e00737.
30. Sarwar, A., Katas, H., & Zin, N. M. Antibacterial effects of chitosan–tripolyphosphate nanoparticles: impact of particle size molecular weight. *Journal of nanoparticle research*, **2014**, *16*(7), 1-14.
31. Al-Jawad, S. M., Taha, A. A., Redha, A. M., & Imran, N. J. Influence of nickel doping concentration on the characteristics of nanostructure CuS prepared by hydrothermal method for antibacterial activity. *Surface Review and Letters*, **2021**, *28*(01), 2050031.
32. Shakir, Z. S., AL-Jawad, S. M., & Ahmed, D. S. Influence of cobalt doping concentration on ZnO/MWCNTs hybrid prepared by sol-gel method for antibacterial activity. *Journal of Sol-Gel Science and Technology*, **2021**,*100*(1), 115-131.
33. Manikandan, A., & Sathiyabama, M. Green synthesis of copper-chitosan nanoparticles and study of its antibacterial activity. *Journal of Nanomedicine & Nanotechnology*, **2015**, *6*(1), 1.
34. Al-Jawad, S. M., Sabeeh, S. H., Taha, A. A., & Jassim, H. A. Synthesis and characterization of Fe–ZnO thin films for antimicrobial activity. *Surface review and letters*, **2019**, *26*(05), 1850197.
35. Syame, S. M., Mohamed, W. S., Mahmoud, R. K., & Omara, S. T. Synthesis of copper-chitosan nanocomposites and their applications in treatment of local pathogenic isolates bacteria. *Orient J Chem*, **2017**, *33*(6), 2959-2969.
36. AL-Jawad, S. M., Sabeeh, S. H., Taha, A. A., & Jassim, H. A. Studying structural, morphological and optical properties of nanocrystalline ZnO: Ag films prepared by sol–gel method for antimicrobial activity. *Journal of Sol-Gel Science and Technology*, **2018**, *87*(2), 362-371.

37. AL-Jawad, S. M., Taha, A. A., & Salim, M. M. Synthesis and characterization of pure and Fe doped TiO_2 thin films for antimicrobial activity. *Optik*, **2017**, *142*, 42-53.